The IRM Quarterly
Spring 2001, Vol. 11, No. 1
Institute for Rock Magnetism

FORC analysis of frozen ferrofluids

Christopher Pike
University of California-Davis

Jim Marvin
IRM

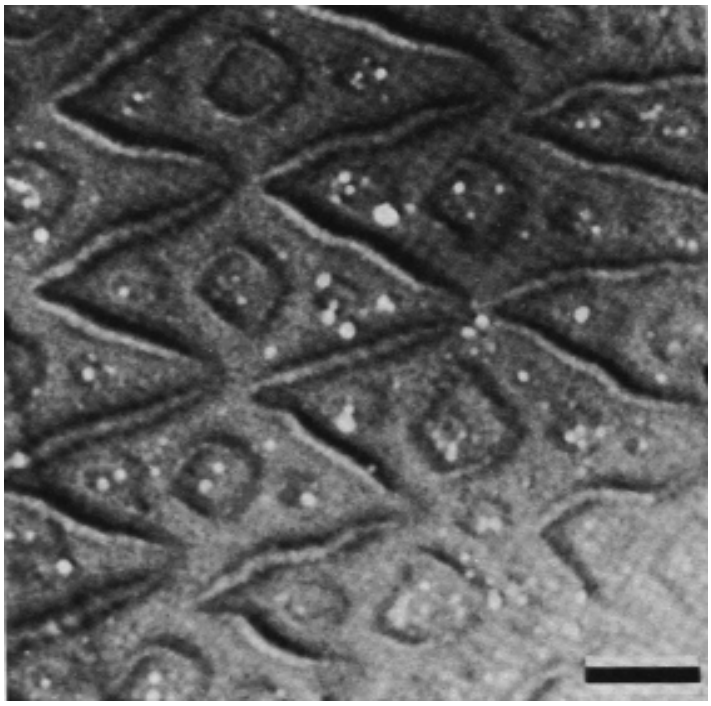

Moskowitz, B. M., Halgedahl, S. L., and Lawson, C. A., 1988, Magnetic domains on unpolished and polished surfaces of titanium-rich titanomagnetite: Journal of Geophysical Research B: Solid Earth, v. 93, p. 3372–3386.

Ferrofluids have been used for magnetic domain imaging since the technique was pioneered by Francis Bitter in the 1930's. High-resolution images such as this (aluminum- and magnesium-substituted titanomagnetite; scale bar = 2.5 μm) are obtained by scanning electron microscopy on dried Bitter patterns.

Ferrofluids are a good example of an interacting single-domain (SD) particle system. A ferrofluid consists of ~10-nm sized magnetite particles immersed in an oil carrier fluid. Surface tension keeps the particles immersed in the fluid. Ferrofluids have several commercial, and even pharmaceutical applications. At room temperature, ferrofluid particles are mobile and superparamagnetic. Below liquid nitrogen temperature, the carrier fluid is frozen and the particles become stable SD. For basic science, ferrofluids have the advantage over other SD systems that their concentration, and hence interaction strength, can be controlled.

In recent years, we have been studying the hysteresis properties of a number of magnetic systems, such as magnetic recording media, permanent magnetic materials (e.g. Alnico), and natural samples. To investigate hysteresis properties, we have employed a class of hysteresis curves known as First Order Reversal Curves (FORCs, see below). To better visualize the information in a set of FORCs, we transform them into a contour plot known as a FORC diagram (described below). A FORC diagram contains much more detailed information about hysteresis properties than the major hysteresis loop or the remanence curves. It can be used to probe subtle variations in magnetic properties that might not be discernable with the conventional hysteresis measurements.

With regard to natural samples, our goal is to use FORC diagrams to obtain information on the distribution of domain states and particle sizes and mineral phases in natural samples, and to gain insight into effects such as thermal relaxation and interparticle interaction. However, natural samples are notoriously complicated systems, and the interpretation of the FORC diagrams of natural samples is commensurately difficult. Therefore, we have tried to develop an interpretational framework starting with more simple and well-behaved samples, such as ferrofluids. We recently performed low-temperature FORC diagram measurements on a ferrofluid at the *IRM*. Before describing our results, we will review the construction of a FORC diagram.

Let us begin with some definitions. The measurement of a First Order Reversal Curve (FORC) begins by saturating a sample in a large positive applied field (see Figure 1). The field is decreased to a reversal field H_r, and the FORC is the magnetization curve that results when the applied field is increased back to saturation [1]. By repeating this measurement for different values of H_r, one obtains a set of curves such as those shown in Figure 2(a). The magnetization at the applied field H_a on the FORC with reversal field H_r is denoted by $M(H_r, H_a)$, where $H_a > H_r$ (see Figure 1). Each individual FORC reflects a combination of reversible (*e.g.*, small displacements of domain walls in an energy well) and irreversible magnetization changes (*e.g.*, displacements of walls through an energy barrier into a different well). The difference between successive FORCs is a consequence of irreversible changes that occur between the successive reversal fields. The FORC distribution, which characterizes in detail the distribution of critical fields for irreversible magnetization changes, is defined as the mixed second derivative:

$$\rho(H_r, H_a) \equiv -\frac{\partial^2 M(H_r, H_a)}{\partial H_r \partial H_a} \qquad (1)$$

where $\rho(H_r, H_a)$ is well defined for $H_a > H_r$. (The notation here is slightly different from that used in our previous work on FORC diagrams [2,3]).

ferrofluids *continued on page 10...*

Editor's Note: This is the second in a series of articles on data analysis and interpretation.

Visiting Fellows' Reports

Investigating the role of microbial versus chemical processes in magnetic mineral formation in soils

Monika Cogoini
University of Oklahoma
Cogoini@ou.edu

Authigenesis of magnetic minerals can occur via abiotic/inorganic as well as various biological processes in soils and sediments. For instance, inorganically-formed ultrafine-grained magnetite was reported from soils in the UK (Maher & Taylor, 1988). The chemical conditions prevailing in soils due to hydrocarbon exposure are also thought to be capable of causing the formation of magnetic phases such as magnetite (Machel, 1996, Machel & Burton, 1991). Alternatively, several types of bacteria can cause magnetic mineral formation either internally in magnetotactic microorganisms (e.g., Bazylinski et al., 1993) or externally by iron-reducing bacteria (e.g., Lovley, 1990, Stolz et al., 1990). The former have been studied in greater detail and the magnetic minerals they produce can be uniquely magnetically characterized because of their specific grain shapes and size range (Bazylinski & Moskowitz, 1997, Moskowitz et al., 1993). In the case of iron-reducing bacteria, the magnetic mineral deposits are dominantly superparamagnetic (SP) magnetite (Moskowitz et al., 1989, Sparks et al., 1990) and are similar to those formed inorganically in soils. The resemblance between inorganically-formed magnetite and magnetic grains formed by iron-reducing bacteria makes it difficult to determine the origin of some magnetic minerals in soils and sediments. Developing a better understanding of microbially-formed magnetic minerals and in particular of the role of iron-reducing bacteria and the conditions under which they produce magnetic minerals is important in order to evaluate their potential contribution to the magnetic signal in soils and geologic deposits. This work investigates biologically-produced magnetic minerals with focus on iron-reducing bacteria as a potentially important factor controlling magnetic mineral formation in soils as compared to chemical processes.

Two soil types were collected in Oklahoma to investigate the formation of magnetic minerals under a variety of laboratory-controlled conditions. The first soil type was collected in two horizontal cores retrieved at depths of 5-12 cm and 15-22 cm. The shallow core consists of a dark grayish-brown silty clayloam that contains decaying plant material. This decaying organic matter appears to be the cause of a coloration change to yellowish along thin layers (usually less than 1 mm) of the soil surrounding the plant material. The soil contained in the deep core is also a silty clayloam, dark grayish- to greenish-brown, and contains less plant material and therefore, there are fewer of the yellowish lenses in the soil. The cores were collected above an aging oil field and the soil is known to have been exposed to hydrocarbons. The second soil is an orange-to-brown clayey loam with abundant ferric iron oxides, which are dominantly hematite.

For the first soil, an array of experiments was set up to test for microbial versus chemical causes for the observed changes in the magnetic signal. Each experiment was conducted by dividing the soil into three:groups: natural samples, positive control samples, and sterile control samples. The natural samples contain the soil as collected in the field. To obtain positive controls, a culture of iron-reducing bacteria known to be capable of producing magnetite was introduced into selected samples of the natural soil. In order to test for a chemical process, samples of the natural soil were sterilized in an autoclave. A total of five sets, each constituting of triplicate (or 4) samples of each of the three groups (natural, positive and sterile controls), were prepared for treatment under five different environmental conditions. Each set was subjected to one of the following treatments: addition of methane, hydrogen, nitrogen, a mixture of methane and oxygen, or oxygen. During the course of approximately 180 days, bulk magnetic susceptibility (χ_b) measurements were conducted periodically and elevation of the magnetic signal generally occurred in biological samples, i.e. natural and positive control samples (Figure 1). The sterile sets showed no consistent increases in the χ_b signal through time, and some drop slightly below the initial χ_b value (Figure 1a and b). The augmentation of χ_b occurs under anaerobic environmental conditions in most of the natural and positive control samples of the shallow core and in many biological samples of the deeper core. The χ_b in natural samples from the shallow core may increase by up to 35 % whereas the χ_b of the deep core samples reaches up to a maximum of 24 %. Only a few of the aerobically treated biological samples (mostly positive control samples of the shallow core) show slightly elevated χ_b. In some samples that showed initial increases in χ_b the signal decreases slightly after prolonged periods of time but remains above the initial χ_b. Several biological samples showing increases in χ_b and their sterile controls were chosen for further analyses at the *IRM* along with an original/untreated soil sample. The main tool for magnetic mineral characterization used at the *IRM* is thermal demagnetization of a saturation magnetization acquired at low-temperature. In addition, other methods including hysteresis and Curie-balance analysis were used on some samples.

Samples from both cores and all groups indicate a somewhat steep initial drop in remanence followed by a more gradual drop upon heating to room temperature and a weakly developed Verwey transition. This is interpreted to indicate the presence of some ultrafine-grained (SP) and coarse (multi-domain)

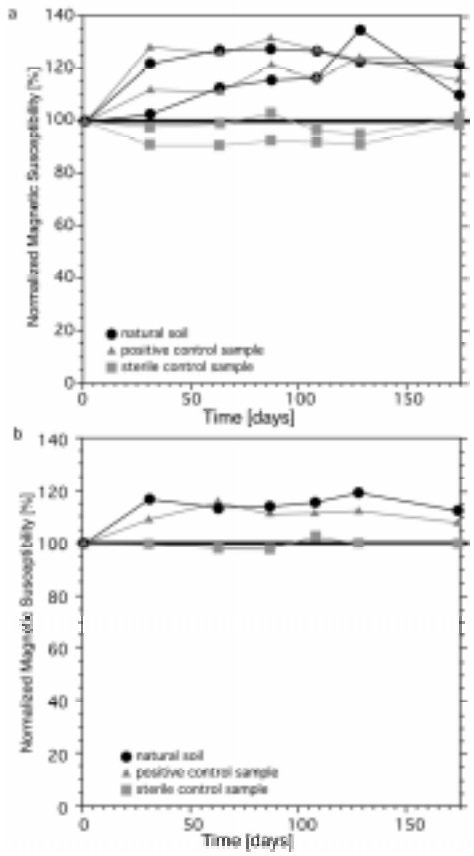

Figure 1. Normalized χ_b for samples of the shallow core: a) treated with methane; b) treated with hydrogen. Biological samples generally show elevated χ_b with time, whereas the magnetic sterilized samples show relatively constant χ_b or occasionally slightly lower values. Standard deviations are commonly less than 5%.

continued on page 6...

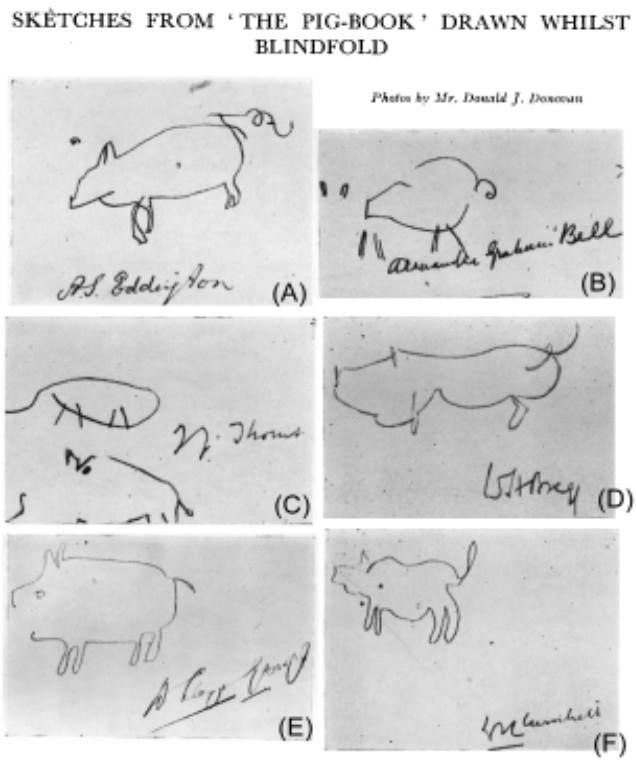

source: The Man of Room 40: The Life of Sir Alfred Ewing, *by A. W. Ewing, 1939, Hutchinson & Co. Ltd., London.*

Guests in the home of Arthur Ewing were invited to sketch a pig while blindfolded. Among the "Pig-Book" sketches are the works of: (A) Arthur Eddington, astronomer and physicist known for his work on the structure and evolution of stars and relativity; (B) Alexander Graham Bell, inventor of the telephone; (C) J.J Thomson, discoverer of the electron and winner of the 1906 Nobel prize for his work on electrical conductivity of gases; (D) William Bragg, who shared the 1916 Nobel prize with his son Lawrence, for their work on x-ray diffraction and crystal structures; (E) David Lloyd George, British Prime Minister from 1916-1922; (F) Winston Churchill, Prime Minister from 1940-45 and 1951-55.

Current Abstracts

A list of current research articles dealing with various topics in the physics and chemistry of magnetism is a regular feature of the IRM Quarterly. *Articles published in familiar geology and geophysics journals are included; special emphasis is given to current articles from physics, chemistry, and materials-science journals. Most abstracts are culled from* INSPEC *(© Institution of Electrical Engineers),* Geophysical Abstracts in Press *(© American Geophysical Union), and* The Earth and Planetary Express *(© Elsevier Science Publishers, B.V.), after which they are subjected to Procrustean editing and condensation for this newsletter. An extensive reference list of articles (primarily about rock magnetism, the physics and chemistry of magnetism, and some paleomagnetism) is continually updated at the* IRM. *This list, with more than 5200 references, is available free of charge. Your contributions both to the list and to the Abstracts section of the* IRM Quarterly *are always welcome.*

Alteration, Diagenesis and Remagnetization

Doh, S.-J., Suk, D.-W., and Kim, B.-Y., 1999, **Paleomagnetic and rock magnetic studies of Cretaceous rocks in the Eumsung Basin, Korea**: *Earth, Planets and Space, v. 51*, no. 5, p. 337-49.
Early Cretaceous red beds and greenish mudstones carry a ChRM that was acquired during or after tilting during late Cretaceous to early Tertiary. Electron microscope observations and rock magnetic experiments show secondary authigenic hematite and magnetite grains of SD-PSD size.

Elmore, R. D., Kelley, J., Evans, M., and Lewchuk, M. T., 2001, **Remagnetization and orogenic fluids: testing the hypothesis in the central Appalachians**: *Geophysical Journal International, v. 144*, no. 3, p. 568-76.
The Helderberg Group, an aquitard, and the Oriskany Formation, a palaeoaquifer, both contain similar, synfolding Late Palaeozoic CRMs residing in magnetite. The Oriskany Formation may have been remagnetized by orogenic fluids, because there is geochemical evidence for the migration of such fluids. In contrast, there is no geochemical evidence for the widespread migration of fluids into the Helderberg Group and thus another remagnetization mechanism, which remains elusive, must be responsible for the Helderberg CRM.

Lewchuk, M. T., Al-Aasm, I. S., Symons, D. T. A., and Gillen, K. P., 2000, **Late Laramide dolomite recrystallization of the Husky Rainbow "A" hydrocarbon Devonian reservoir, northwestern Alberta, Canada: paleomagnetic and geochemical evidence**: *Canadian Journal of Earth Sciences, v. 37*, no. 1, p. 17-29.
Middle Devonian carbonates here contain a well-defined ChRM, residing in SD to PSD magnetite, of Middle Eocene to Middle Miocene age. Four generations of dolomite are recognized, and all have similar isotopic compositions ($\delta^{18}O$ of -10.7 to -16.5% (PDB), $\delta^{13}C$ of +0.7 to +3.2% (PDB), and Sr ratios of 0.70826 to 0.70846) that do not match Devonian carbonate or seawater values. These data indicate that mixed pre-Laramide basinal fluids, heated by burial during the Laramide Orogeny, were present when the dolomites were recrystallized and (or) precipitated prior to petroleum migration and accumulation in the reservoir.

Richter, C., Hayashida, A., Guyodo, Y., Valet, J. P., and Verosub, K. L., 1999, **Magnetic intensity loss and core diagenesis in long-core samples from the East Cortez Basin and the San Nicolas Basin (California Borderland)**: *Earth, Planets and Space, v. 51*, no. 5, p. 329-36.
High-resolution (1-2 cm interval) magnetic measurements made on about 180 m of continuous U-channel samples from two Leg 167 cores showed that by ca. 4-6 months after the cores were drilled , the magnetic intensity had decreased to 7%-10% of the initial magnetization. Both cores were strongly affected by the decay of a metastable magnetic mineral or the dissolution of fine-grained magnetite by organic matter reduction. Nevertheless we were able to define a stable characteristic remanence for most of the core.

Yamazaki, T., Solheid, P. A., and Frost, G. M., 2000, **Rock magnetism of sediments in the Angola-Namibia upwelling system with special reference to loss of magnetization after core recovery**: *Earth, Planets and Space, v. 52*, no. 5, p. 329-36.
These Leg 175 sediments have a high total-organic-carbon content and very low concentrations of ferrimagnetic minerals. Severe and rapid loss of remanent magnetization occurred during storage, with less than 10% of the initial intensity remaining a after a few months. Decreases in S-ratio suggest preferential loss of magnetite, and hysteresis parameters and ARM/SIRM ratios suggest preferential dissolution of finer grains. Low-temperature magnetometry revealed the presence of magnetite in the sediments even after the completion of sulfate reduction.

Anisotropy

Yaouancq, G., and MacLeod, C. J., 2000, **Petrofabric investigation of gabbros from the Oman ophiolite: comparison between AMS and rock fabric**: *Marine Geophysical Researches, v. 21*, p. 3-4.
From the paleo-Moho to the top of the foliated gabbros level, 73% of the rocks display a good correspondence in orientation, between the magnetic and rock fabric orientation. AMS is controlled by secondary magnetites located in the fracture network of the olivines, and probably, but to a lesser extent, by secondary magnetites located in the exsolution lamellae of the clinopyroxenes. The magnetic foliation is constrained by the orientation of the olivine fracture planes, which is in turn constrained by the orientation of the overall magmatic rock fabric. No correlation between the shape and magnitude of the AMS and plagioclase fabrics can be established

Carriers and Origins of NRM

Turner, G. M., 2001, **Toward an understanding of the multicomponent magnetization of uplifted Neogene marine sediments in New Zealand**: *Journal of Geophysical Research, v. 106*, no. B4, p. 6385-97.
The NRM consists of three components: (1) a low (<150° C) T_b component interpreted to be a recent TVRM; (2) an intermediate (150-250° C) T_b component, thought to be all that remains of the primary DRM; and (3) a high (>250° C) T_b component that is considered to be diagenetic in origin. Rock magnetic data which show that specimens carrying strong high T_b components have a distinctly different spectrum of ferrimagnetic grains, specifically a population with much higher coercivities than is seen in specimens which lack a high T_b component. It is argued that these high-coercivity, high T_b grains are secondary in origin, leading to the conclusion that the intermediate T_b component is the primary detrital magnetization.

continued on page 4...

Yoshida, M., Khan, I. H., and Ahmad, M. N., 1998, **Remanent magnetization of oolitic ironstone beds, Hazara area, Lesser Himalayan thrust zone, northern Pakistan: its acquisition, timing, and paleoenvironmental implications**: *Earth, Planets and Space, v. 50*, no. 9, p. 733-44.
Chamosite-hematite type oolitic ironstone is distributed in the Cretaceous-Tertiary (K-T) boundary zone. Ferromagnetic properties are dominated by fine-grained hematite that formed from iron hydroxides during early diagenesis. The ChRM direction indicates that the magnetization was acquired during Early Paleocene time. The initial Fe-rich sediments were deposited under anoxic conditions, probably in a non-marine or brackish environment. During early diagenesis, after development of oolitic textures, the paleoenvironment became arid, and the CRM was acquired through the conversion of amorphous hydroxides or goethite to fine-grained hematite.

Data Processing and Analysis

Oda, H., and Shibuya, H., 1998, **An improvement in ABIC-minimizing deconvolution for continuously measured magnetic remanence data**: *Earth, Planets and Space, v. 50*, no. 1, p. 15-22.
Deconvolution of magnetic remanence which has been continuously measured along a long-core sample is improved by eliminating the disturbance of severe intensity variation confined to a narrow layer. The deconvolution is constrained by the smoothness of the magnetization measured by the L_2-norm of second order difference. The previous model uses a single smoothness parameter for the entire sample and the optimum smoothness is obtained by minimizing ABIC (Akaike's Bayesian information criterion), while an additional parameter is introduced in the modified scheme for a layer where intensity fluctuation is strong. The modified deconvolution scheme was applied to 5-mm interval magnetic remanence data for two sections of ODP Hole 767B. We assumed another smoothness for the uppermost 1.5 cm of Section 767B-6H1 where the coring disturbance is severe. For Section 767B-6H2, the Australasian microtektite layer (108-113 cm), where the magnetization intensity shows a strong peak, is expressed by a different smoothness parameter from other part. In both cases the minimum ABIC was lowered and the calculated error was reduced, demonstrating the improvement of the model by incorporating additional information other than magnetic remanence data in the prior distribution of the data.

Tsunakawa, H., Okada, M., and Niitsuma, N., 1999, **Further application of the deconvolution method of post-depositional DRM to the precise record of the Matuyama-Brunhes reversal in the sediments from the Boso Peninsula, Japan**: *Earth, Planets and Space, v. 51*, no. 3, p. 169-73.
The Matuyama-Brunhes geomagnetic reversal was continuously recorded in massive siltstones with a time resolution better than 9 years. However the Boso sediments probably have post-depositional detrital remanent magnetization (pDRM) depressing short-period variations due to the convolution of the geomagnetic field. The previous application of the deconvolution method of pDRM to the 900 year records gave a half fixing depth of 21 cm. Further application of this fixing depth to the 4100 year record clearly shows nearly 100 year variations in both of the inclination and declination.

Utada, H., Neki, M., and Kagiyama, T., 2000, **A study of annual variations in the geomagnetic total intensity with special attention to detecting volcanomagnetic signals**: *Earth, Planets and Space, v. 52*, no. 2, p. 91-103.
A model is proposed in which changes in magnetization of near-surface rocks due to seasonal changes in atmospheric temperature produce annual variations in geomagnetic total intensity. First, amplitude and phase difference of annual variations in the total intensity and ground temperature data were determined by time series analyses. Considering thermal diffusion from the surface into the ground, the phase difference was converted to a characteristic depth, and then the amplitude of annual temperature variation at the depth was estimated. Finally, the observed total intensity variations were compared with the expected change on the basis of the temperature dependence of the rock magnetization measured in the laboratory, and good agreement was found. Correction of annual variations by using temperature data will enable more accurate detection of volcanomagnetic signals.

Environmental Magnetism

Abdul-Razzaq, W., and Gautam, M., 2001, **Discovery of magnetite in the exhausted material from a diesel engine**: *Applied Physics Letters, v. 78*, no. 14, p. 2018-19.
Magnetite was detected in the particulate matter collected from diesel engine exhaust using a total exhaust dilution tunnel. This discovery is important in terms of the health effects of exposure to magnetite or its interaction with static magnetic fields or low-frequency electromagnetic fields. Magnetite is the best absorber of microwave radiation of any biological material in the 0.5-10 GHz frequency range through the process of electromagnetic resonance. This includes the frequencies that are normally used in the cellular telephone industry.

Evans, M. E., 2001, **Magnetoclimatology of aeolian sediments**: *Geophysical Journal International, v. 144*, no. 2, p. 495-7.
In the classic sites of the Chinese Loess Plateau, soil formation during interglacials leads to magnetic enhancement in the palaeosols. In other regions (Alaska, Siberia), magnetic susceptibility peaks during glacial intervals. A simple qualitative analysis based on density sorting determines the regimes under which one or the other dominates. Published data permit a certain degree of quantification, and lead to the conclusion that proximal sites are likely to manifest Alaskan/Siberian-type magnetoclimatological patterns. Beyond a few hundred kilometres, however, distal sites will be dominated by Chinese-type patterns.

Fukuma, K., and Torii, M., 1998, **Variable shape of magnetic hysteresis loops in the Chinese loess-paleosol sequence**: *Earth, Planets and Space, v. 50*, no. 1, p. 9-14.
The shape of magnetic hysteresis loops varies with susceptibility χ. When the ratio of the ferrimagnetic (FM) to antiferromagnetic (AFM) contribution is relatively low (low χ), the broad loop is controlled by lithogenic FM and AFM minerals. For samples with intermediate χ, constricted loops originate from the addition of a broad loop from the lithogenic fraction and a narrow loop from a pedogenic fraction with high superparamagnetic content. Then with further χ increase, the constricted shape almost disappears and the loop is dominated by the pedogenic fraction.

Heslop, D., Langereis, C. G., and Dekkers, M. J., 2000, **A new astronomical timescale for the loess deposits of Northern China**: *Earth and Planetary Science Letters, v. 184*, no. 1, p. 125-39.
A refined timescale for the entire sequence of Quaternary Chinese loess relies upon the correlation of detailed monsoon records to the astronomical solution of Laskar (1990) and the oceanic ODP677 $\delta^{18}O$ record of Shackleton et al. (1990). The chronological scheme considers in detail the relative structures of the palaeoclimatic and palaeomagnetic records to produce an accurate timescale that is consistent with the current understanding of loess depositional and post-depositional processes. Analysis of this chronological framework demonstrates downward displacement of the palaeomagnetic horizons with respect to the climatic record.

Extraterrestrial Magnetism

Gunnlaugsson, H. P., 2000, **Analysis of the magnetic properties experiment data on Mars: results from Mars Pathfinder**: *Planetary and Space Science, v. 48*, no. 15, p. 1491-504.
Spectral data for the material adhering to the magnets, as well as the time dependence of magnetic dust accumulation, are the basis of a new model of the magnetic properties of the dust. Optical reflection spectra of the magnetic dust differ slightly from the reflection of ground soil/dust in the vicinity of the lander. Magnetic dust has been removed from the magnets at least twice during the 80 sol mission by wind gusts, in a manner similar to sand blasting. A lower limit for the saturation magnetisation of the most magnetic particles is found to be 5 Am^2/kg.

Kletetschka, G., Wasilewski, P. J., and Taylor, P. T., 2000, **Mineralogy of the sources for magnetic anomalies on Mars**: *Meteoritics & Planetary Science, v. 35*, no. 5, p. 895-9.
The intense magnetic anomalies on Mars are likely due to TRM and possible carriers include SD and MD magnetite, hematite, and pyrrhotite. The intensity of TRM (in 0.05 mT) is in descending order: SD magnetite, SD pyrrhotite, MD hematite, MD pyrrhotite, MD magnetite, SD hematite. Each of these minerals is used in a thin sheet model to estimate the concentrations required to generate the observed magnetic anomaly (1500 nT at 100 km altitude) assuming TRM acquisition in a 0.05 mT magnetic field.

Taylor, A. P., Barry, J. C., and Webb, R. I., 2001, **Structural and morphological anomalies in magnetosomes: possible biogenic origin for magnetite in ALH84001**: *Journal of Microscopy, v. 2720*, no. 2001, p. 0022-2720.
We report biogenic magnetite whiskers resembling the magnetite whiskers detected in the Martian meteorite ALH84001 by Bradley et al., and interpreted by those authors as evidence of vapour-phase (abiogenic) growth. The structures of the magnetite particles in ALH84001, their spatial arrangement and coprecipitation with carbonates and proximity to silicates are all consistent with being biogenic. Electron-beam-induced flash-melting of magnetosomes produced numerous screw dislocations in the {111}, {100} and {110} lattice planes and induced fusion of platelets. From this, the lack of screw dislocations reported in the magnetite particles in ALH84001 (McKay et al., and Bradley et al.) indicates that they have a low-temperature origin.

Instruments and Measurements

Leslie, K. E., Binks, R. A., Lewis, C. J., Scott, M. D., Tilbrook, D. L., and Du, J., 2001, **Three component spinner magnetometer featuring rapid measurement times**: *IEEE Transactions on Applied Superconductivity, v. 11*, no. 1, p. 252-5.
The remanent magnetisation of rock specimens is measured using a high temperature superconductor rf SQUID. Samples are rotated around two orthogonal axes to facilitate the calculation of the three-component remanence vector with a minimum of operator intervention. Measurements of remanence ranging from 10^{1} to 10^{-5} A/m, with errors of $1*10^{-5}$ A/m, have been achieved in measurement times of 20 s, in a typical geophysical laboratory environment.

Magnetic Field Records and Paleointensity Methods

Harrison, C. G. A., 2001, **Resource Letter: G-1: Geomagnetism**: *American Journal of Physics, v. 69*, no. 5, p. 534-42.
This Resource Letter provides a guide to the literature on the internally generated geomagnetic field. The topics covered include the origin of the geomagnetic field and the energy requirements and core properties necessary for its generation; a description of the geomagnetic field, including its spherical harmonic representation, and its rates of change, as well as models of the secular variation; observations of the field relevant to paleomagnetism and continental drift; information about magnetic anomalies in the oceans, sea floor spreading and plate tectonics; reversals of the geomagnetic field and magnetochronology.

Tarduno, J. A., Cottrell, R. D., and Smirnov, A. V., 2001, **High geomagnetic intensity during the mid-Cretaceous from Thellier analyses of single plagioclase crystals**: *Science, v. 291*, no. 5509, p. 1779-83.
The authors report data from 56 Thellier-Thellier experiments on plagioclase crystals separated from basalts of the Rajmahal Traps of India that formed during the Cretaceous Normal Polarity Superchron. These data suggest a time-averaged paleomagnetic dipole moment of $12.5\pm1.4*10^{22}$ Am^2, three times greater than mean Cenozoic and Early Cretaceous-Late Jurassic dipole moments when geomagnetic reversals were frequent. This result supports a correlation between intervals of low reversal frequency and high geomagnetic field strength.

Magnetization Processes

Katari, K., and Bloxham, J., 2001, **Effects of sediment aggregate size on DRM intensity: a new theory**: *Earth and Planetary Science Letters, v. 186*, no. 1, p. 113-22.
Inter-particle attractions due to electrostatic or van der Waals forces, or biologically mediated flocculation, lead to the formation of aggregates, which prevent the settling of individual magnetic grains. Viscous drag becomes important for large clay-magnetite aggregates, which can be tens of micrometers in diameter, and larger magnetic fields are necessary to bring their moments into alignment. A new model of DRM acquisition assumes a log-normal size distribution of flocs, all of which have the same magnetic moment. The undersaturation of magnetic intensity in laboratory DRM experiments is explained by the larger viscous drag encountered by the larger aggregates which prevents perfect alignment with the applied magnetic field.

Kosterov, A., 2001, **Magnetic hysteresis of pseudo-single-domain and multidomain magnetite below the Verwey transition**: *Earth and Planetary Science Letters, v. 186*, no. 2, p. 245-54.
Hysteresis loops have been measured as a function of temperature between 10 K and room temperature for two size fractions of crushed magnetite: 1-5 μm (pseudo-single-domain, PSD) and 100-150 μm (multidomain, MD). The material under study appears to be fairly close to stoichiometric magnetite, with a Verwey transition temperature of 115 K for the MD sample and 118 K for the PSD sample. For both samples, hysteresis properties below the Verwey transition depend critically on whether or not the samples were cooled through the transition in the magnetic field. For the PSD sample, an even more complex behavior has been observed: temperature dependences of coercive force obtained after zero-field-cooling differ significantly for the demagnetized versus magnetized starting magnetic state.

Maksimochkin, V. I., 2000, **The pressure effect on the magnetization of basalts**: *Izvestiya, Physics of the Solid Earth, v. 36*, no. 7, p. 565-70.
The effect of pressure application time on the formation of the pressure-induced viscous remanent magnetization (PVRM) in basalts is studied. The PVRM at P=160 MPa is shown to be 1.8 to 7.3 times higher than the viscous remanent magnetization. The pressure effect on the PVRM process in basalts with Z=0.4-0.75 single-phase oxidation of titanomagnetites is 2 to 4 times higher than the similar effect in titanomagnetites that were not oxidized or experienced high-temperature multi-phase oxidation.

Spinu, L., Srikanth, H., Wiemann, J. A., Li, S., Tang, J., and O'Connor, C. J., 2000, **Superparamagnetism and transverse susceptibility in magnetic nanoparticle systems**: *IEEE Transactions on Magnetics, v. 36*, no. 5, p. 3032-4.
The temperature and field dependence of the transverse susceptibility (χ_T) of a magnetic nanoparticle system has been investigated. The T- dependence is found to exhibit characteristic features that can be related to relaxation behavior in nanoscale magnetic systems. The experimental data are interpreted using a modified coherent magnetization rotation model based on a two level approach.

Stinnett, S. M., and Doyle, W. D., 2000, **Relationship between the intrinsic thermal switching field at 10^{-9} s and the anisotropy field in magnetic recording media**: *IEEE Transactions on Magnetics, v. 36*, no. 5, p. 2456-8.
New measurements of the anisotropy field from rotational hysteresis are compared with previous measurements of the intrinsic switching field in a variety of particulate and thin film media. All of the particulate media have intrinsic switching fields of $H_0 \sim H_K/3$ independent of particle size or orientation. In contrast to the particulate samples, the thin film samples have a larger ratio of H_0/H_K from 0.5 to 0.8 possibly indicating a change in reversal mode from incoherent to coherent rotation. Further, results on γ-Fe_2O_3 particulate samples confirm that below a few nanoseconds, thermal switching ceases to drive the increase in $H_{CR}(t)$.

Modeling and Theory

Muxworthy, A. R., 2001, **Effect of grain interactions on the frequency dependence of magnetic susceptibility**: *Geophysical Journal International, v. 144*, no. 2, p. 441-7.
Magnetic susceptibility and κ_{fd} have been modelled for weakly interacting assemblages of SD magnetite grains, near the SP - stable SD threshold known as the blocking volume, v_b. Weak interactions between SP grains effectively increase the anisotropy, which reduces v_b, causing a decrease in the peak values of κ_{fd}, by over 50 per cent for certain grain distributions. However, it is also found that the reduction of v_b as a result of interactions can actually increase κ_{fd} for certain grain distributions.

Shcherbakov, V. P., Lamash, B. E., and Sycheva, N. K., 2000, **The magnetic susceptibility and viscous magnetization of interacting single-domain grains**: *Izvestiya, Physics of the Solid Earth, v. 36*, no. 5, p. 430-6.
Numerical calculations based on Boltzmann statistics for an ensemble of single-domain (SD) particles, with volume concentration ranging from c = 0 to 5%, show that magnetostatic interaction has virtually has no effect on the equilibrium value of the susceptibility. The calculations also show that interaction significantly affects viscous behavior at c≥0.5%, due to the drastic broadening of the relaxation time spectrum as

abstracts *continued on page 8...*

continued from page 2

magnetite (Figure 2). A comparison of the low-temperature analysis of a natural sample that was exposed to methane and which was later subjected to additional treatment in the laboratory to enhance the growth of iron-reducing bacteria is shown in Figure 2 (inset). The thermal demagnetization curves reveal a general shift towards higher remanence at room temperature, an increased drop of remanence upon heating through the Verwey transition, and a slight shift of remanence loss towards higher temperatures after the additional treatment. These results could indicate growth and/or further production of magnetite in the soil after enhancing for iron-reducing bacteria. If growth of the magnetite occurred, this could also explain the observed decrease in the χ_b measurements after prolonged times in some of the biological samples since coarser magnetite has lower χ_b than SP grains. Hysteresis measurements on a hydrogen exposed natural and a sterile control sample indicate that the ferrimagnetic χ is responsible for most of the χ_b signal (99.9% and 99.2% of χ_b for the natural and sterile sample, respectively). All Curie-balance measurements had very low signal to noise ratios due to the small sample sizes and relatively low concentrations of magnetic material. No additional magnetic phases were identified within the soil by any of the methods used. The rock-magnetic results indicate that small amounts of magnetite of various grain sizes were originally present in the soil and magnetite continues to grow in the biological, i.e. natural and positive control samples. The results also show that chemical processes alone are not capable of furthering the production of magnetic minerals under the conditions provided in the experiments.

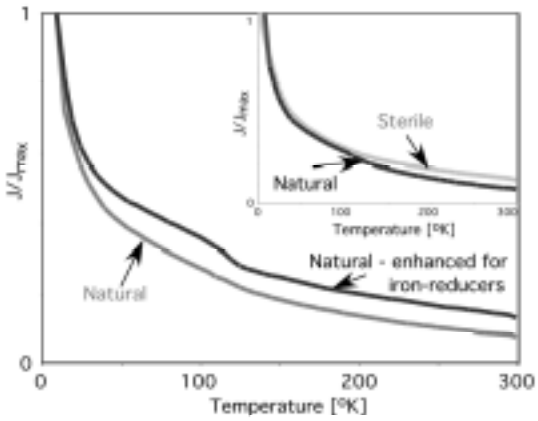

Figure 2. *Thermal demagnetization of low-temperature SIRMs. Inset: comparison of a hydrogen-treated natural and a sterile control sample shows minor differences, and both suggest the presence of some SP grains and small amounts of MD magnetite in the original soil. The sterilized sample shows only a very weakly developed Verwey transition, which can be recognized more easily in the first derivative (not shown here). The other two curves represent a methane-treated natural sample and a methane-treated sample after enhancing the amount of iron-reducing bacteria present. The additional treatment of the sample possibly resulted in a coarsening of the magnetite grains present.*

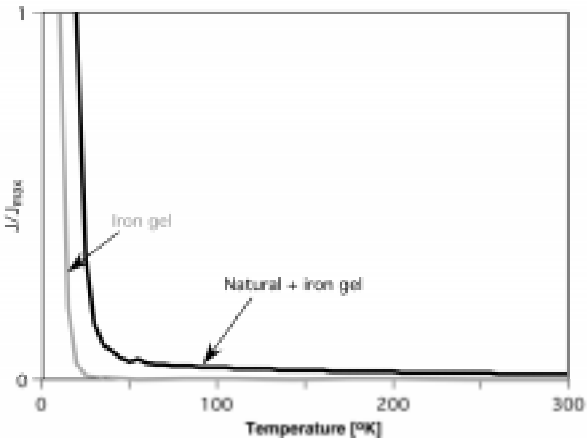

Figure 3. *Thermal demagnetization of low-temperature SIRMs for an iron-gel sample (ferric oxy-hydroxide) and a natural sample treated with the iron-gel to enhance growth of iron-reducing bacteria present in the soil. Although the SIRMs were acquired at slightly different temperatures, the demagnetization patterns are similar in having steep initial drops. The iron-gel sample loses its remanence within a temperature range of 10 - 15°. The natural sample carries some remanence up to at least 200K. The additional remanence-carrying material present in the soil could be ultrafine-grained magnetite.*

One of the remaining unresolved issues is: why are the differences noticed mainly in the coarse magnetite rather than the SP fraction despite the increases in the χ_b? Iron-reducing bacteria are known to produce SP-sized magnetite. Is it possible that the bacterial magnetite rapidly aggregates to coarser magnetite under favorable conditions for growth of iron-reducing bacteria – or are the conditions prevailing in the microcosms favorable for inorganic growth of the magnetite once a nucleus has formed via biologic pathways?

The second soil type that was investigated is an orange-brown clayey loam with abundant ferric iron oxides, which are dominantly hematite. This soil was initially treated in the laboratory to enhance the amount of iron-reducing bacteria present within the soil and the experiment was monitored by χ_b measurements. The results showed rapid initial increases in the χ_b signal, which tripled within less than 80 days, and a concurrent color change from orange-brown to black suggesting the presence of magnetite. However, further analyses of the magnetic mineralogy at the IRM using thermal demagnetization of a saturation remanence acquired at low-temperature, hysteresis measurements, Curie-balance analysis, pARM, and Mössbauer spectroscopy showed inconclusive results. The low-temperature thermal decay pattern of a treated natural sample was compared to that of a ferric oxy-hydroxide sample, the material added to the soil in order to enhance the growth of iron-reducing bacteria (Figure 3). The low-temperature curve of the ferric oxy-hydroxide sample shows a very steep initial drop in remanence and it retains no remanence at temperatures above approximately 15°K. The natural soil sample initially loses its remanence rapidly, but it carries a small amount of remanence up to higher temperatures. Similar to the ferric oxy-hydroxide sample, the natural sample has almost no magnetic remanence at room temperature. These results may indicate the presence of extremely ultrafine-grained magnetite (few nm) in the natural soil, the formation of which may have been caused by iron-reducing bacteria. However, it is also possible that some of the ferric oxy-hydroxide that is used to enhance the growth of iron-reducing bacteria changed to a ferric iron component of different crystallinity during the course of the experiment which may show somewhat different demagnetization patterns. All other methods used in an attempt to decipher the magnetic mineralogy within the soil were unconvincing. Additional experiments on the clayey loam to test for a microbial versus chemical process of magnetic mineral formation were set up in the laboratory prior to my visit at the IRM. These experiments were inconclusive with regard to the χ_b behavior of most samples, which is probably due to the low initial values inherent in this soil type. Further investigations on this soil type were not conducted because of the difficulties encountered in determining the magnetic mineralogy and the weak initial χ_b signal. The observed enhancement in the χ_b in the initial experiment is probably due to the fact that ferric iron was introduced to the soil in a readily bioavailable form, i.e. the ferric iron in the compound is easily utilized by microorganisms such as iron-reducing bacteria. Since the natural soil contains mainly hematite, a poorly bioavailable ferric iron compound of high crystallinity, magnetic mineral formation could be either very slow or not occurring even under conditions that otherwise could sustain the growth of iron-reducing bacteria. Based on the results presented, it appears that the first soil type described above is favorable for biological production of magnetic minerals, probably via iron-reducing bacteria. The presence of abundant organic material (in

this case plant material and hydrocarbons) and bioavailable ferric iron are probably the key factors for enabling microbial magnetic mineral formation. The additional growth of magnetite grains could be caused either by bacteria or an inorganic process, which probably required the presence of previously formed magnetite.

My visit at the IRM was of great value from a scientific as well as from a personal viewpoint. I am very grateful for the opportunity of visiting such an exceptional place. I wish to express my sincere appreciation to all members of the IRM for their support not only concerning the technical aspects but also for the many interesting discussions and helpful suggestions. And at last, but not the least, I would like to acknowledge Ann Hirt for her friendship and for the many valuable and inspiring discussions we had during the long working nights spent at the institute.

References

Bazylinski, D.A., and Moskowitz, B.M., 1997, Microbial biomineralization of magnetic iron minerals: *Reviews in Mineralogy, v. 35*, p. 181-223.

Bazylinski, D.A., Heywood, B.R., Mann, S., and Frankel, R.B., 1993, Fe3O4 and Fe3S4 in a bacterium: *Nature, v. 366*, p. 218.

Lovley, D.R., 1990, Magnetite formation during microbial dissimilatory iron reduction, in Frankel, R.B. and Blakemore, R.P., eds., Iron Biominerals: New York, Plenum Press, p. 151-166.

Machel, H.G., 1996, Magnetic contrasts as a result of hydrocarbon seepage and migration, in Schumacher, D. and Abrams, M.A., eds., Hydrocarbon migration and its near-surface expression: *AAPG Memoir, v. 66*, p. 99-109.

Machel, H.G., and Burton, E.A., 1991, Cause and spatial distribution of anomalous magnetization in hydrocarbon seepage environments: *American Association of Petroleum Geologists Bulletin, v. 75*, p. 1864-1876.

Maher, B.A., and Taylor, R.M., 1988, Formation of ultrafine-grained magnetite in soils: *Nature, v. 336*, p. 368-370.

Moskowitz, B.M., Frankel, R.B., and Bazylinski, D.A., 1993, Rock magnetic criteria for the detection of biogenic magnetite: *Earth and Planetary Science Letters, v. 120*, p. 283-300.

Moskowitz, B.M., Frankel, R.B., Bazylinski, D.A., Jannasch, H.W., and Lovley, D.R., 1989, A comparison of magnetite particles produced anaerobically by magnetotactic and dissimilatory iron-reducing bacteria: *Geophysical Research Letters, v. 16*, p. 665-668.

Sparks, N.H.C., Mann, S., Bazylinski, D.A., Lovley, D.R., Jannasch, H.W., and Frankel, R.B., 1990, Structure and morphology of magnetite anaerobically-produced by a marine magnetotactic bacterium and a dissimilatory iron-reducing bacterium: *Earth and Planetary Science Letters, v. 98*, p. 14-22.

Stolz, J.F., Lovley, D.R., and Haggerty, S.E., 1990, Biogenic magnetite and the magnetization of sediments: *Journal of Geophysical Research, v. 95*, p. 4355-4361.

FUNDAMENTAL ROCK MAGNETISM AND ENVIRONMENTAL APPLICATIONS CONFERENCE

Erice, Italy - 26 June to 1 July 2002

http://www.sicily.infcom.it/uk/localita/TP/erice/fotografie/castelli/erice3.html

Focus: This conference is a joint initiative of the "**Mag-Net**" European Network for Mineral Magnetic Studies of Environmental Problems and the **Institute for Rock Magnetism**. Updated reviews, new observations on nano-phase to submicron magnetic particles and examples of successful inter-disciplinary problem-solving will be given by keynote speakers, together with poster presentations of current research by participating scientists. Significant time will be kept for open discussion on data interpretation, supported by short oral input from participants.

Location: The Conference will be held at the "Ettore Majorana" Foundation and Centre for Scientific Culture (EMFCSC, http://www.ccsem.infn.it/) in the historic and artistic town of Erice, Italy, located at the western end of Sicily. Participants should arrive on Wednesday, June 26, and depart in the afternoon of Monday, July 1. The cost of the conference is US$500. This includes all food and lodging for 5 days and nights, meeting costs (e.g. registration, abstract book, ice-breaker, coffee breaks, conference dinner), transportation to/from Palermo airport and one field excursion.

Participation: There is space for a maximum of 100 participants and 20 accompanying persons, with priority to those who register early and who plan to stay for all conference sessions. We especially encourage application of PhD students and young (< 36 years) researchers. The objective is to have 50% of PhD students and young researchers and 25% of invited senior speakers. The cost of the conference may be partly covered with external funding (i.e. EC, NSFS.) with priority to young researchers.

Applications: Obtain forms from **Pierre Rochette** (rochette@cerege.fr) or **Silvia Nardi** (nardi_s@ingv.it).

Deadlines: - response to first circular by September 30, 2001 - selection of conference applicants if required (by November 1, 2001) - submission of extended abstracts by December 31, 2001 (maximum 2 pages and 1 figure) to be published in a book of abstracts edited by the Istituto Nazionale di Geofisica e Vulcanologia, Rome, Italy.

compared with the case of noninteracting particles.

Oceanic Crust Magnetism

Nazarova, K. A., Wasilewski, P. J., and Dick, H. J. B., 2000, **Magnetic study of serpentinized harzburgites from the Islas Orcadas Fracture Zone**: *Marine Geophysical Researches, v. 21*, no. 5, p. 475-88.
Magnetite in these serpentinites is variably maghemitized, shown by optical microscopy, thermomagnetic analyses and low temperature cycling of SIRM. Hysteresis ratios fall in a restricted range regardless of coercivity. The apparent grain size configured in a three dimensional vein network plus maghemitization might be responsible for this observation. Maghemitization does not affect thermal magnetic stability and enhances the geophysical importance of remanence in serpentinites, which may be very important for generation of long wavelength aeromagnetic and possibly even satellite magnetic anomalies.

Zhou, W., Van der Voo, R., Peacor, D. R., Wang, D., and Zhang, Y., 2001, **Low-temperature oxidation in MORB of titanomagnetite to titanomaghemite: A gradual process with implications for marine magnetic anomaly amplitudes**: *Journal of Geophysical Research, v. 106*, no. B4, p. 6409-21.
Electron microscopic and rock magnetic studies indicate that the degree of oxidation of titanomagnetite in MORB increases only gradually with sample age. The envelope of data in a z versus age plot can be represented by $z=p+q \log t$, where $p \approx 0.38$, $q \approx 0.38$, and t is in millions of years (for t>100 ka). The rate of maghemitization is controlled by many factors on both macroscopic and microscopic scales, including regional oceanic crustal structures, lithological features, grain size, and surrounding matrices. The NRM intensity of MORB varies as a function of age, concentration and grain size of magnetic materials, and the degree of alteration.

Paleomagnetism & Tectonics

Tarduno, J. A., and Smirnov, A. V., 2001, **Stability of the Earth with respect to the spin axis for the last 130 million years**: *Earth and Planetary Science Letters, v. 184*, no. 2, p. 549-53.
Recently continental paleomagnetic data rotated into a hotspot reference frame have been used to suggest the Earth rotated 18° with respect to the spin axis at 110 Ma. The authors test this true polar wander (TPW) hypothesis using paleomagnetic data from widespread granitic rocks of cratonal North America. These data conflict with TPW predictions leading to rejection of the hypothesis. The calculated polar displacement is instead consistent with motion of the Atlantic hotspots during the mid-Cretaceous. This analysis suggests that the time-averaged position of the spin axis has deviated by no more than 5° over the last 130 million yr, indicating that mantle mass heterogeneities have not changed rapidly enough to drive TPW.

Synthesis and Properties of Magnetic Minerals

Ayub, I., Berry, F. J., Bilsborrow, R. L., Helgason, O., Mercader, R. C., Moore, E. A., Stewart, S. J., and Wynn, P. G., 2001, **Influence of zinc doping on the structural and magnetic properties of α-Fe_2O_3**: *Journal of Solid State Chemistry, v. 156*, no. 2, p. 408-14.
Zinc-doped α-Fe_2O_3 has been prepared by hydrothermal methods. The zinc K-edge EXAFS and interatomic potential calculations indicate that Zn^{2+} ions substitute for Fe^{3+} ions in the lattice and are accompanied by oxygen vacancies. The ^{57}Fe Mossbauer spectra recorded between 296 and 18 K demonstrate that the Morin transition in α-Fe_2O_3, is completely suppressed within this temperature range by the presence of zinc. The ^{57}Fe Mossbauer spectra recorded in situ at temperatures between 300 and 915 K show the material to undergo conversion to the spinel-related $ZnFe_2O_4$ phase in this temperature regime.

de Boer, C. B., and Dekkers, M. J., 2001, **Unusual thermomagnetic behaviour of haematites: neoformation of a highly magnetic spinel phase on heating in air**: *Geophysical Journal International, v. 144*, no. 2, p. 481-94.
A magnetic phase with T_C~475° C is formed during routine thermomagnetic analysis of various haematites. The formation temperature can be as low as 400° C for synthetic samples, whereas temperatures of 700-800° C are required for natural samples. The new phase has a cubic spinel structure with unit cell a_0=0.8350±0.0005 nm, similar to pure maghemite. The low T_c of this particular maghemite variety suggests that the vacancy (and/or cation) ordering is different from typical maghemite; a cation-deficient structure with part of the vacancies on tetrahedral sites is suggested. Thermally activated release of incorporated hydroxyl groups would trigger the formation of maghemite traces on the surface of well-crystalline haematite planes. The formation of traces of this highly magnetic mineral during routine stepwise thermal demagnetization or during annealing haematite at high temperatures may seriously affect NRM measurements or may be erroneously taken as haematite's defect moment.

Fan, R., Chen, X. H., Gui, Z., Liu, L., and Chen, Z. Y., 2001, **A new simple hydrothermal preparation of nanocrystalline magnetite Fe_3O_4**: *Materials Research Bulletin, v. 36*, no. 3, p. 497-502.
Nanocrystalline magnetite particles have been prepared by hydrothermal reaction of ferrous sulfate ($FeSO_4$), sodium hydroxide and sodium thiosulfate ($Na_2S_2O_3$) at 140° C. The X-ray powder diffraction pattern indicates that the product is single-phase magnetite in an inverse cubic spinel structure. Its composition is determined by traditional chemical analysis combined with X-ray photoelectron spectroscopy. Transmission electron microscopy images show that the magnetite particles are homogenous in the shape of quasi-sphere polyhedra with an average diameter of 50 nm.

Garcia, J., Subias, G., Proietti, M. G., Blasco, J., Renevier, H., Hodeau, J. L., and Joly, Y., 2001, **Absence of charge ordering below the Verwey transition temperature in magnetite**: *Physical Review B, v. 63*, no. 5, p. 054110.
The electronic state of Fe_3O_4 below the Verwey transition has been studied by X-ray resonant scattering at the iron K edge of the forbidden (0 0 2) and (0 0 6) reflections. These reflections are permitted by the anisotropy of the iron anomalous scattering factor. The energy and the azimuthal angle dependence of the intensity of these reflections do not change above and below the transition temperature. Moreover, the spectrum at low temperature does not change upon orientation of the crystal c axis. The results clearly show that no charge ordering of Fe^{3+} and Fe^{2+} occurs in the insulating phase of magnetite.

Zysler, R. D., Vasquez-Mansilla, M., Arciprete, C., Dimitrijewits, M., Rodriguez-Sierra, D., and Saragovi, C., 2001, **Structure and magnetic properties of thermally treated nanohematite**: *Journal of Magnetism and Magnetic Materials, v. 224*, no. 1, p. 39-48.
The effect of thermal treatment on the structure and magnetic properties of α-Fe_2O_3 rhombohedrical nanoparticles (30 nm) synthesized by chemical route has been analyzed by XRD, TEM, magnetization measurements and Mossbauer spectroscopy. Annealing of these samples recrystallizes the nanoparticles maintaining their mean size while changing the crystalline anisotropy energy, thus leading to an increase of the spin reorientation Morin temperature and changes in the superparamagnetic-blocking behavior.

MAGNETIC INDUCTION IN IRON AND OTHER METALS

BY

J. A. EWING

M.A., B.SC., F.R.SS.L. AND E., M.INST.C.E.,

PROFESSOR OF MECHANISM AND APPLIED MECHANICS IN THE UNIVERSITY OF CAMBRIDGE.

LONDON:
"THE ELECTRICIAN" PRINTING AND PUBLISHING COMPANY, LIMITED,
SALISBURY COURT, FLEET STREET, E.C.

1892.

CHAPTER V.

MAGNETIC HYSTERESIS.

§ 77. Magnetic Hysteresis.-The curves which have been drawn to show the effects of cyclic magnetising processes in iron, steel, nickel, and cobalt, have this important feature in common, that there is a tendency on the part of the metal to persist in any magnetic state which it may have acquired. This tendency is specially obvious whenever an alteration begins to be made in the character of the magnetising process. Thus, when the magnetising force has been raised to its highest value, we find, on beginning to reduce the force, that the magnetism tends to remain. It does not all remain, but the rate at which it disappears during withdrawal of the magnetising force is notably less than the rate at which magnetism was being acquired during imposition of the force, especially at the beginning of the withdrawal. The existence of residual magnetism when the force is wholly withdrawn is one result of this reluctance on the part of the metal to change its magnetic condition. But the results of this tendency go further. If, for example, after withdrawing the magnetising force, we begin to re-apply it, we find in the early stages of the process the same reluctance to change; the metal begins to regain magnetism, but not so fast as it was losing magnetism during the last stages of the removal of the force. The rate, however, improves, and when the force has been completely restored we find that the piece has recovered all, or nearly all (sometimes even a little more than all), the magnetism it lost while the force was being withdrawn. The curve of magnetisation comes again to the same, or nearly the same, point as that from which it started; but its path during the process of return differs entirely from its path during removal of the force. The two curves form a loop, and any intermediate value of the magnetic force is associated with different values of the magnetisation during the two processes.

Moreover, this description applies equally to the effects of *any* cyclic variation of magnetic force, provided the range through which the force is varied be not exceedingly small. Starting from any condition of magnetism and of magnetising force, if we remove and re-apply a part of the force, or if we apply and remove a supplementary force, and repeat the process until its effects become cyclic, we find that the two stages of the process may be represented by two curves, which do not coincide, but differ in a way that may be concisely described by saying that there is a tendency, at each change of process, for the preceding magnetic condition to persist. The changes of magnetism lag behind the changes of force. This tendency has received the name of *magnetic hysteresis*, from υστερω, to lag behind.*

* *Proc.* Roy. Soc., No. 216, 1881, p.22; *Phil. Trans.*, 1885, p.524.

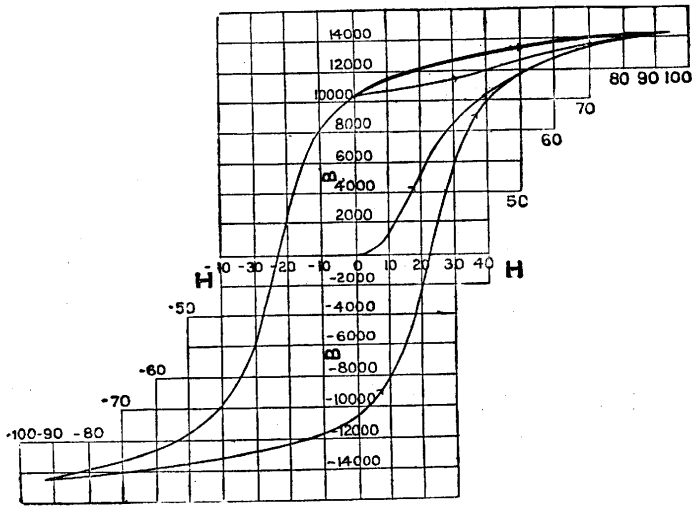

FIG. 35.—Pianoforte Steel Wire, annealed.

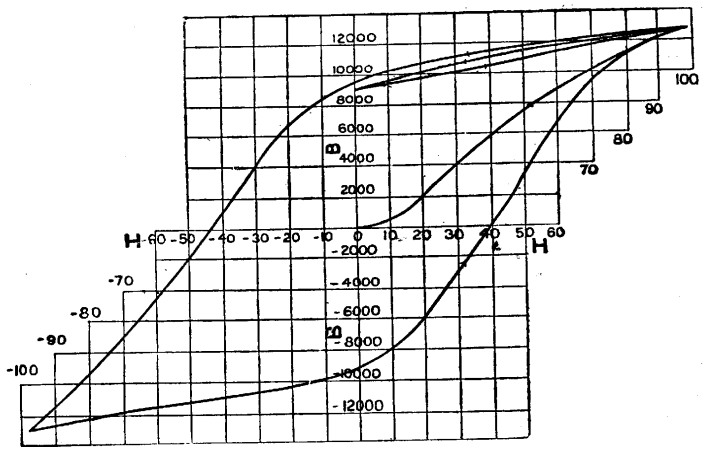

FIG. 36.—Pianoforte Steel Wire, glass-hard.

continued from page 1

When a FORC distribution is plotted, it is convenient to change coordinates from $\{H_r, H_a\}$ to $\{H_c = (H_a - H_r)/2, H_b = (H_a + H_r)/2\}$. A FORC diagram is a contour plot of a FORC distribution with H_b and H_c on the vertical and horizontal axes, respectively. Since $H_a > H_r$, then $H_c > 0$, and a FORC diagram is confined to the right-hand half plane. In Figure 2(b) we show the FORC diagram calculated from the data in Figure 2(a). The H_c coordinate is referred to as the microcoercivity.

To explain the motivation for this mixed second derivative and change of coordinates, it is necessary to give a brief introduction to the Preisach model. Let us begin by defining a simple mathematical construction referred to as a hysteron. As shown in Figure 3, the hysteron $\gamma_{\alpha\beta}$ equals 1 for large values of H, switches to -1 when H falls below H_α, and remains at -1 until H rises above H_β. The FORC distribution for $\gamma_{\alpha\beta}$ is a point delta function which has an infinite peak at $H_r = H_\alpha$ and $H_a = H_\beta$, and which equals zero elsewhere. In H_c and H_b coordinates, $\rho(H_r, H_a)$ will consist of a point delta function at $H_c = (H_\alpha - H_\beta)/2$, $H_b = (H_\alpha + H_\beta)/2$. However, $(H_\alpha - H_\beta)/2$ is just the half-width of $\gamma_{\alpha\beta}$, which corresponds to its coercivity, and $(H_\alpha + H_\beta)/2$ is the horizontal offset of $\gamma_{\alpha\beta}$, which we refer to as its bias (see Figure 3). Hence, on a FORC diagram, the H_c and H_b coordinates of the point delta function give the coercivity and bias, respectively, of $\gamma_{\alpha\beta}$.

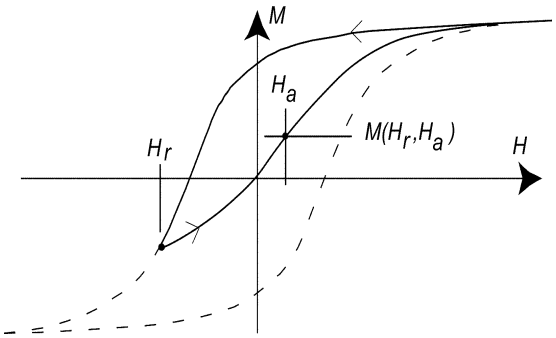

Figure 1. The measurement of a First Order Reversal Curve (FORC) begins with saturation by a positive field. The field is ramped down to a reversal field H_r. The FORC consists of a measurement of the magnetization as the field is then increased from H_r back up to saturation. The magnetization at applied field H_a on the FORC with reversal point H_r is denoted by $M(H_r,H_a)$. The dotted line represents the major hysteresis loop. The FORC with a reversal field at negative saturation is equivalent to the lower half of the major hysteresis loop.

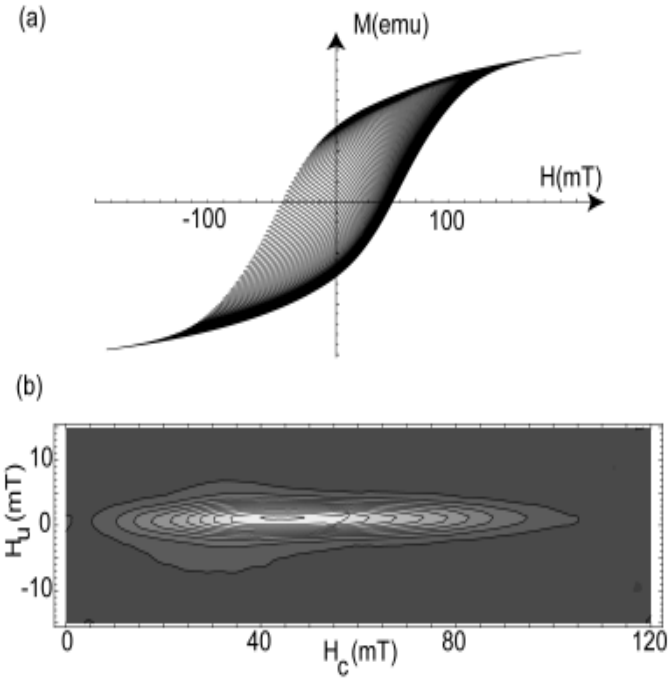

Figure 2. (a) FORC data for Yucca Mountain ash flow tuff sample, from southern Nevada. (b) A FORC diagram for above data (SF = 2).

In the Preisach model, hysteresis is generated by the superposition of a collection of hysterons with a distribution of coercivities and biases, where the distribution of coercivities and biases is referred to as a Preisach distribution, $P(H_c, H_b)$. By a simple extension of the above- described result with one hysteron, it can be shown that the FORC distribution $\rho(H_r, H_a)$ for such a collection of hysterons will be equivalent to $P(H_c, H_b)$. Whenever a hysteresis system can be rigorously described by the Preisach model (*i.e.*, as the superposition of hysterons), the FORC and Preisach distributions will be equivalent.

The Preisach model was first suggested as a model of hysteresis in interacting SD particle systems. In this model, each hysteron represents an individual particle in the assemblage. The coercivity of a hysteron corresponds to the coercivity of a SD particle if it were isolated from the system. The bias of a hysteron corresponds to a fixed interaction field, which represents the interaction of an individual particle with the surrounding assemblage of particles. The Preisach distribution corresponds to a distribution of particle coercivities and interaction fields. Therefore, the motivation for the mixed second derivative and change of coordinates is that, at least in this simple model, the FORC distribution $\rho(H_r, H_a)$ will be equivalent to the Preisach distribution and to a distribution of particle coercivities and interaction fields.

In real interacting single domain particles systems, hysteresis is more complex and rich than can be described by a simple superposition of hysterons, so the Preisach model must be considered as a phenomenological construction to describe hysteresis in an approximate way. Similarly, the interpretation of a Presiach distribution as a distribution of coercivities and interaction fields is only valid in an approximate way. And the Preisach distribution associated with a specific system is not uniquely specified or well-defined. In contrast to the Preisach distribution, the FORC distribution is always well-defined for any magnetic system. The FORC distribution $\rho(H_c, H_b)$ is defined using only a set of measured FORC data, a second derivative, and a change of coordinates. Its definition is not dependent on the Preisach model, or any other theoretical model.

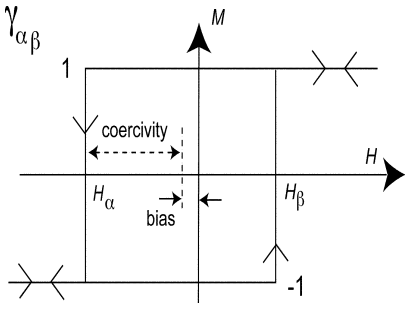

Figure 3. The hysteron $\gamma_{\alpha\beta}$ equals 1 for large values of H, switches to -1 when H falls below H_α, and remains at -1 until H rises above H_β. The half width of the hysteron is its coercivity, and the horizontal offset of its center is referred to as its bias.

The details of data acquisition and analysis involved in obtaining a FORC distribution have been described in detail elsewhere [2,3]. A certain amount of numerical smoothing is inherent in the calculation of a FORC diagram from experimental data: this is quantified by a smoothing factor (SF), which can vary between 2 for the highest quality data and 5 for poor quality data. Figure 2 shows both typical FORC data and the FORC diagram for a well-characterized sample of Yucca Mountain ash flow tuff, from southern Nevada, which consists of weakly interacting SD particles [4]. The fact that the distribution in Figure 2(b) is narrowly confined to the centre horizontal axis is characteristic of weakly interacting SD particles.

At the IRM we measured, for the first time, FORC diagrams on a Vibrating Sample Magnetometer at low temperatures. The ferrofluid, produced by Ferrofluidics, Inc., comes with extra carrier fluid which can be added to dilute the particle concentration. We studied it in the concentration out of the bottle, 0.2 emu/mL, and at roughly a 10 to 1 dilution. The results, shown in Figure 4, are satisfying in that they confirm many aspects of FORC diagrams and SD particle models. Note in both the undiluted and diluted samples that decreasing temperature pushes the distribution peak to higher coercivity. At low enough temperature, this distribution would be well separated from the vertical axis, like the distribution in Figure 2; the fact that even at 5 K the ferrofluid

Ewing, (James) Alfred

b. March 27, 1855, Dundee, Scotland
d. Jan. 7, 1935, Cambridge, England

Sir Alfred is credited with discovering and naming the phenomenon of hysteresis. A student and protegé of Fleeming Jenkin at Edinburgh, Ewing went on to professorships in mechanical engineering in Tokyo, Ediburgh and Cambridge. His wife, née Annie Washington, was great-great grand niece of the first US president. Ewing wrote numerous papers on the effects of stress on magnetization, and several books, including *The Steam Engine and Other Heat Engines* (1885) and *Magnetic Induction in Iron* (1892). His research also included work on cryptography, seismology, and thermoelectric effects.

distribution meets the vertical axis indicates that a large fraction of the system is still unblocked at 5 K.

Notice that the degree of vertical spread is greater for the undiluted case. This confirms that, to a first order, the vertical spread is a measure of a distribution of interaction fields. Furthermore, the degree of vertical spread in the undiluted sample is relatively constant from 5 to 9 to 12 K, while the distribution of microcoercivities shifts substantially. This indicates that, to a first order, the strength of interactions is independent of the particle coercivities and temperature, which is a satisfying result.

The darkest shaded regions of these plots correspond to negative values of the FORC distribution. At the right hand side of these diagrams, there are randomly fluctuating negative regions. This is primarily a result of noise. We have chosen a contour line close to a zero value of the distribution. As a result, when the distribution gets close to zero, noise can produce spurious crossings of the zero contour boundary line, which gives rise to random fluctuations of the dark shading. However, at 5 and 9 K, for the diluted sample, there is a negative region in the lower left hand corner which is not just noise. Weakly negative regions are, in fact, commonly observed in FORC diagrams, which is one aspect of these diagrams that separates them from Preisach diagrams.

Finally, an interesting result with the undiluted sample is a secondary peak located at the diagram origin, and to the left of the main peak. At first sight, this peak might seem to indicate some kind of bimodal particle distribution. But we have shown theoretically that this secondary peak arises when the distribution crosses the stable/superparamagnetic threshold. The interesting thing for us it that this secondary peak is spread out vertically by the interactions in the undiluted sample.

The ferrofluid studied here is a well-behaved and well understood system, and not necessarily of interest to geologists. However, as we gain experience with FORC diagrams in these simple systems, we will be better able to apply FORC diagrams to more complicated natural systems.

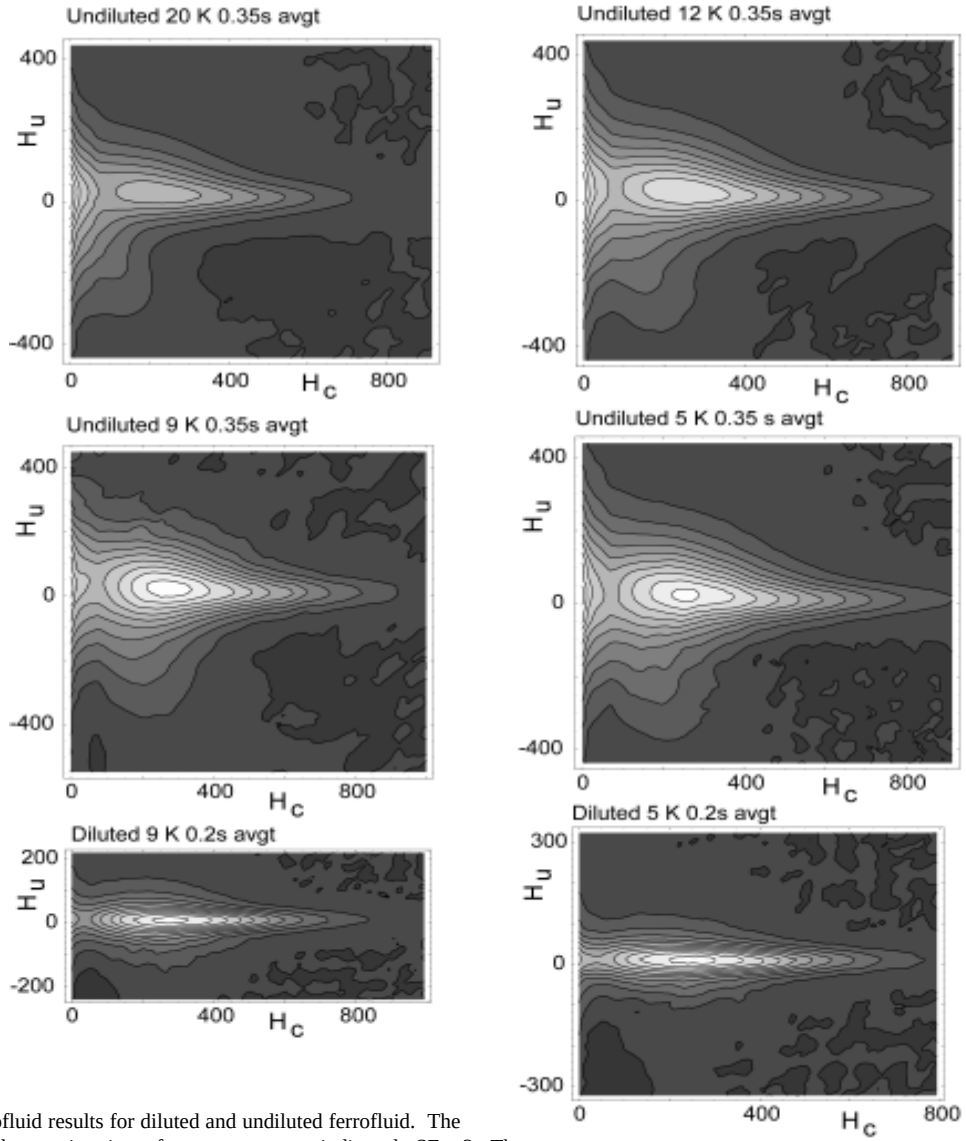

Figure 4. Ferrofluid results for diluted and undiluted ferrofluid. The temperature and averaging time of measurement are indicated. SF = 3. The greater vertical spread of the undiluted sample indicates stronger interactions. Increased temperature shifts the distribution to lower microcoercivities.

References

1. Mayergoyz, I.D., Mathematical models of hysteresis, *IEEE Trans. Magn.*, *MAG-22*, 603-608, 1986.
2. Pike, C.R., A.P. Roberts, and K.L. Verosub, Characterizing interactions in fine magnetic particle systems using first order reversal curves, *J. Appl. Phys.*, *85*, 6660-6667, 1999.
3. Roberts, A.P., C.R. Pike, and K.L. Verosub, FORC diagrams: A new tool for characterizing the magnetic properties of natural samples, *J. Geophys. Res., in press*.
4. C.M. Schlinger, D.R. Veblen and J.G. Rosenbaum, Magnetism and magnetic mineralogy of ash flow tuffs from Yucca Mountain, Nevada, *J. Geophys. Res. B, 96*, 6035–6052, 1991

The *Institute for Rock Magnetism* is dedicated to providing state-of-the-art facilities and technical expertise free of charge to any interested researcher who applies and is accepted as a Visiting Fellow. Short proposals are accepted semi-annually in spring and fall for work to be done in a 10-day period during the following half year. Shorter, less formal visits are arranged on an individual basis through the Facilities Manager.

The *IRM* staff consists of **Subir Banerjee**, Professor/Director; **Bruce Moskowitz**, Associate Professor/ Associate Director; **Jim Marvin**, Senior Scientist; **Mike Jackson**, Senior Scientist and Facility Manager, and **Peat Solheid**, Scientist.

Funding for the *IRM* is provided by the **National Science Foundation**, the **W. M. Keck Foundation**, and the **University of Minnesota**.

The *IRM Quarterly* is published four times a year by the staff of the *IRM*. If you or someone you know would like to be on our mailing list, if you have something you would like to contribute (*e.g.*, titles plus abstracts of papers in press), or if you have any suggestions to improve the newsletter, please notify the editor:

Mike Jackson
Institute for Rock Magnetism
University of Minnesota
291 Shepherd Laboratories
100 Union Street S. E.
Minneapolis, MN 55455-0128
phone: (612) 624-5274
fax: (612) 625-7502
e-mail: irm@geolab.geo.umn.edu
www.geo.umn.edu/orgs/irm/irm.html

I R M

Institute for Rock Magnetism

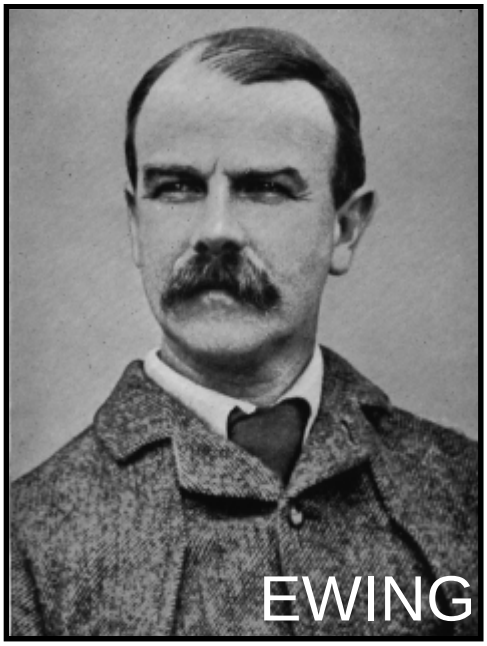

Collector's Series #21

source: The Man of Room 40: The Life of Sir Alfred Ewing, *by A. W. Ewing, 1939, Hutchinson & Co. Ltd., London.*

The IRM Quarterly

University of Minnesota
291 Shepherd Laboratories
100 Union Street S. E.
Minneapolis, MN 55455-0128
phone: (612) 624-5274
fax: (612) 625-7502
e-mail: irm@geolab.geo.umn.edu
www.geo.umn.edu/orgs/irm/irm.html

Nonprofit Org.
U.S Postage
PAID
Mpls., MN
Permit No. 155